

## Kinetic, Equilibrium and Thermodynamic Study for Adsorptive Detoxification of Pb<sup>+2</sup> By Thiocarbamoyl Chitosan

ANURAG CHOUDHARY\*, SARDAAR SINGH POONIA and ANURAG KADAWASARA

Department of Chemistry, JNV University, Jodhpur, India.

### Abstract

The environmental effect of industrial effluents, including chromium (Cr), lead (Pb), mercury (Hg), copper (Cu), and nickel (Ni) can have harmful impacts, which includes soil, water, and air pollution, bioaccumulation in food chains, degradation of ecosystems, loss of biodiversity, and contaminated drinking water. Biopolymers such as chitosan have been widely used in wastewater treatment. The ability of thiocarbamoyl chitosan to remove lead ions was assessed by combining thio urea and glutaraldehyde (GLA). During the first two hours of interaction with sorbent, 86% of the metal ions were shown to have been eliminated. According to the adsorption investigation, the prepared sorbent had an outstanding removal rate of metal ions, with a Langmuir maximum absorption capacity of 38 mg/gm at 25 degrees Celsius and a pH of 6. With a linear coefficient of 0.9996, the data on adsorption kinetics were predicted using a pseudo-second order kinetic model. The Langmuir isotherm, which suggests favourable adsorption by homogenous monolayer adsorption, might represent the adsorption process effectively. The adsorption procedure was also demonstrated to be exothermic at all temperatures, with spontaneous responses being energetically endorsed as indicated by negative free energy values.



### Article History

Received: 20 February 2023

Accepted: 15 June 2023

### Keywords

Chitosan;  
Equilibrium Isotherm;  
Industrial Effluents;  
Kinetics.

### Introduction

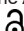
The advancement of industrialization and modern civilization in recent decades has seriously and irreparably impaired the global ecosystems.<sup>1</sup> Due to their persistence in the environment and worrisome accumulation in both aquatic and terrestrial ecosystems, industrial pollutants are particularly detrimental.<sup>2</sup>

The production of steel, leather, plastics, metallurgy, paper, textiles and fabrics, paints, and pigments, electroplating, cement, wood preservatives are kind of industrial products where heavy metals are extensively utilized. Generally, the wastewater discharged from these enterprises contains metal ions lead Pb (II), chromium Cr (VI), copper Cu (II), nickel Ni (II), mercury Hg (II) and other elements,

**CONTACT** Anurag Choudhary ✉ anurag051981@gmail.com 📍 Department of Chemistry, JNV University, Jodhpur, India.



© 2023 The Author(s). Published by Enviro Research Publishers.

This is an  Open Access article licensed under a Creative Commons license: Attribution 4.0 International (CC-BY).

Doi: <https://dx.doi.org/10.12944/CWE.18.2.11>

which are key contributors to environmental contamination.<sup>3</sup> Lead is one of the nonferrous metals that is utilised extensively and discarded as industrial effluents in aforementioned industries. When these products are manufactured or used, lead can be released into the environment. Lead is now found in almost every aspect of modern life, including our diets, our drinking supplies, and even our air. Airborne lead aerosol is a widespread environmental hazard. Largest source of naturally occurring lead include volcanic ash and soil dust. Lead is not a significant cause of poisoning when it is present in its elemental form, unlike certain other metals like mercury.

The presence of lead in drinking water posed to serious concern worldwide. The US Geological Survey anticipated that 14.5 million metric tonnes of lead will be produced globally in 2021.<sup>4</sup> Degradation of the ancient lead-based plumbing systems (such as lead solder and leaded brass) is what leads to substantial levels of Lead (II) in drinkable water.<sup>5</sup>

WHO and US-EPA lead (II) guidelines for drinking water are 10 and 15 g/L, respectively. Abortions, stillbirths, infertility, foetal deaths, and developmental delays or intellectual disabilities may result from Pb (II) exposure over and above these recommendations.<sup>6</sup>

A great number of economically developed nations have created cutting-edge inventions, which includes vacuum evaporation, ion exchange, crystallization, solvent extraction, and membrane process technologies, for the purpose of eliminating these industrial toxicants.<sup>7,8</sup>

Adsorption techniques have emerged as the most flexible and distinguishing way for establishing their superiority over other conventional processes because of its simple mechanism, low expense, high reliability, and simple access to a large variety of adsorbents.<sup>9</sup>

Natural polymers have been studied extensively over the last several decades, and a variety of strategies have been developed to increase their ability to bind metals. Many scientists and researchers concentrated on finding readily accessible and affordable biomaterials for wastewater remediation. Some of the well-known natural polymers have

drawn a lot of interest for this purpose, including chitosan,<sup>10</sup> alginate,<sup>11</sup> cellulose,<sup>12</sup> lignin,<sup>13</sup> and starch.<sup>14</sup>

Polysaccharides from plants like *Proopis Cineraria* leaves have been used to effective elimination of some ground water contaminants.<sup>15</sup> Bio-sorption is recommended since it produces little to no secondary pollution when bio resources are treated as adsorbents. Other essential characteristics are the capacity to regenerate and reuse the adsorbent and to recover the adsorbate metal ions. Since it has been known that adsorption is one of the best and simplest ways to treat wastewater, researchers have consistently worked to create adsorbents that are affordable, efficient, eco-friendly, and repeatable. In order to better understand the adsorption properties of chitosan and its derivatives, a lot of work is being done in this area. Due of their interaction with metal cations, biopolymers like chitosan have been studied in great detail. These biosorbents have been successfully used to separate heavy metals from industrial wastewater in both their natural and chemically modified forms.<sup>16</sup> By alkaline N deacetylating chitin, chitosan is a naturally occurring polycationic polymer that has good metal-binding properties and is biocompatible and biodegradable. Chitosan polymer consists poly (amino saccharide) containing poly (1-4)-2-amino-2-deoxy-D-glucose monomers. It is amenable to the addition of additional functional groups because it has a high fraction of hydroxyl and amine groups. It is often chemically modified with both hydroxyl and amino groups to increase stability and improve its capacity to chelate heavy metal ions.<sup>17</sup>

Sulphur, a soft binding element, has a notable attraction towards many heavy metals that are soft acids and may create a persistent metal-sulphur complex, in accordance with the HSAB (hard - soft acids- bases) hypothesis proposed by Pearson<sup>18</sup> in 1963, which was used to predict complexation processes.<sup>19</sup> Interest has been generated by thiourea (TH) with extra amino groups. Thiourea sequesters by attaching to metal ions. To create sorbents that trap metal ions, chitosan and TH were utilised. Pengcheng *et al.* (2010) found that reduced sorption kinetics and equilibrium occurred after more than 6 hours.<sup>20</sup> Additionally, several of them showed limited sorption capacity and decreased efficiency when the



### Study on Influence of Solution pH

Metal sorption study was carried out at regulated pH range (1.0 to 8.0) at 25 °C by continuous shaking of 100 ml metal ions (5mg/L) solution with load of 1.0 gm of prepared template at 150 rpm for 12 h. The chosen pH was regulated with 0.1 M HNO<sup>3</sup> and 0.1 M NaOH. Upon completion, lead (II) content in aqueous solution was measured.

### Adsorption study of lead by TCCS (Thiocarbamoyl Chitosan)

Each batch experiment trial employed a specified amount of 100 mL aqueous solutions of Lead (II) ion in a 250 mL glass stoppered Erlenmeyer flask and different volumes of adsorbent was tested for adsorption for a predetermined contact of 120 minutes at atmospheric temperature. To establish adsorption equilibrium, the mixture is continually agitated on a rotator shaker set to 150 RPM. After reaching equilibrium, these mixtures were taken from the flask, filtered through a micron filter, and the supernatant was tested for the presence of any remaining metal ions. For each experiment, the whole test was conducted in triplicate with a variation of less than 1% and only means data were used. Figure 1 depicts the whole method.

The reducing efficiency (%) and uptake capacity (mg/g) of a distinctive study were evaluated through the underlying equations No 1 and 2 respectively.

$$\text{Removal effectiveness (\%)} = \frac{C_i - C_t}{C_i} \times 100 \quad \dots(1)$$

$$\text{Adsorption ability (mg/g)} = \frac{C_i - C_t}{m} \times V. \quad \dots(2)$$

Where *m* is the adsorbent weight (gm), *V* is entire volume of batch under treatment (L), and *C<sub>i</sub>* is the original metal content (mg/L). Residual metal ion content (mg/L) at time *t* (min) was referred as *C<sub>t</sub>*.

### Study for Adsorption Isotherm

The adsorption constants calculated from different models provide essential insight into the adsorption process and adsorbent affinities. Several types of equilibrium isotherm have been developed to describe adsorption relationships. However, because of simplicity, good experimental fits data, widely applicability and interpretability, the Langmuir and Freundlich isotherm hypothesis, two of the most popular in the field, were used to correlate the relationship for adsorption capacity and liquid

phase concentration. It is common practise to apply linear regression to choose an appropriate isotherm and evaluate its usefulness.

Adsorption equilibrium was assessed by specified initial metal ion quantities (2-10 mg/L). Adsorption trials were carried out for agitation time of 150 minutes for 100 ml aqueous solution of metal ions in 250 ml glass stoppered flask at different temperature ranges of 25, 35, 45 and 55 °C with the input of 1.0 mg adsorbent. A thermostat water bath shaker at 120 RPM was used for all the experiments keeping solution pH at 6.0. Later, the MP-AES method was used to quantify metal ion concentration to calculate absorption capacity. Experimental statistics were practiced to satisfy two distinct models in origin pro 8.5 software. Higher linear coefficient (R<sup>2</sup>) and smaller standard statistical error (SSE) are indicators of the finest-fitted isotherm.

As suggested by the Langmuir, a mono-molecular stack will be adsorbing onto a surface with a finite number of evenly charged adsorptive sites. The Freundlich principle may be utilized to achieve multilayer adsorption on surfaces with different strengths, even when such surfaces are heterogeneous.<sup>11</sup>

### Adsorption Kinetics Study

There are various types of kinetic model used in adsorption studies but due to straightforward applicability, good interpretations of experimental data which allows for perspective into the underlying sorption procedure and wide applicability in adsorption systems, lagergren pseudo-first and pseudo-second order kinetic designs seemed used to predict the rate and mechanism of metal sorption.

A kinetic inspection was carried out by taking 1.0 gm of TC-CS in a flask containing of Pb<sup>+2</sup> ions (100 ml, 5 mg/L) by fixing the solution pH at 6.0. The flask's contents were shaken at 150 rpm at 25 °C. 5 ml solution from reaction mixture was extracted at predefined intervals (0, 5, 10, 15, 20, 25, 30, 60, 90, 120 min.) and measured for Pd (II) concentration.

kinetic parameters are used to validate experimental results and study the governing strategy of adsorption phenomenon including mass transfer and chemical reaction. The chemical reaction of functional binding sites on the surfaces of the

adsorbent and adsorbate provides the basis for adsorption. With the use of the experimental data from the investigating study, pseudo-first order and pseudo-second order kinetic models developed by Lagergren were used to estimate the rate and mechanism of metal adsorption.

**Error Analysis**

Error analysis for the nonlinear curve fits was carried out in order to identify the theoretical kinetic and isotherm models that best match the experimental kinetic and equilibrium data. Using the Origin Pro software 8.1 computer programme, the correlation index ( $R^2$ ) and the sum of square errors (SSE) were computed in accordance with eqs. No. (3) and (4)

$$R^2 = 1 - \frac{\sum(q_{exp} - q_{fit})^2}{\sum(q_{exp} - q_{mean})^2} \dots(3)$$

where  $q_{fit}$  is the expected value of  $q_{exp}$  for the theory under investigation. The better fit of a model is the one with  $R^2$  closer to 1.0.

$$SSE = \sum(q_{exp} - q_{fit})^2 \dots(4)$$

The smaller values of SSE, can be consider to be optimal fit of the model under investigation.

**Results and Discussion**

**Batch Adsorption studies**

TC-CS in varied amounts was used to conduct a conventional adsorption investigation. Metal ion concentration was taken at 5 mg/L at room temperature with shaking for 2 hours at 150 RPM on orbital shaker at pH 6. The adsorption results showed that the metal sorption had increased by up to 86.8% with raising adsorbent amount from 0.01 g to 5 g. The results are shown in Figures 2 and 3. It was shown that after the adsorbent dosage exceeded 5 gm, there were no appreciable improvements in solubility.

The obtained trend is based on the fact that boosting adsorbent amount offers more binding centres for adsorption. Additionally, it was shown that percentage removal initially rises noticeably from 0.01 to 2 gm, but above 5 gm of dosage, no obvious change in extraction percentage was observed, which is caused by active site overlapping. The capacity actually decreases at doses exceeding 5 mg and beyond because more adsorption sites on

the adsorbent remain unsaturated with increased dosage amounts. This comes after earlier findings that were documented in the literature.<sup>24</sup>

Figure 5 (a and b) illustrates SEM (Scanning Electron Microscopy) images of produced TCCS and lead-adsorbed TCCS, respectively. The surface micrograph of the adsorbent material had a rugged and flaky appearance with pores and micro interspaces that was coated with lead ions thru physical and chemical sorption.

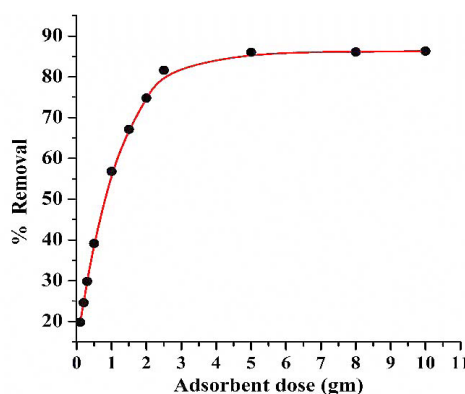


**Fig. 2: Percentage removal of lead by TCCS dose**

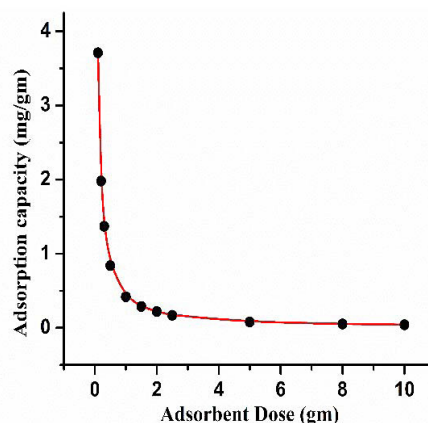


**Fig. 3: Removal capacity for lead by TCCS dose**

**Influence by Solution pH**

Image 4 represents about influence of pH on removal capacity of adsorbent for  $Pb^{+2}$  ions. It was observed that uptake capacity was increased with pH value up to 6 and thereafter it was gradually plateaued in the range of 6-8 and then declined at higher pH. This is because of the nature of net charge type on the

adsorbent surface. At lower pH, insignificant uptake of metal ions was attributed due to partial protonation of active sites which leads to weaker electrostatic interaction. A chelation mechanism was proposed for increased uptake capacity at moderate pH levels.

As  $pH_{zpc}$  is found to be 7.5, it was expected that the uptake amount should be increased but actually, it has been found to be lower due to the precipitation of hydroxide in basic medium.<sup>23,25</sup>

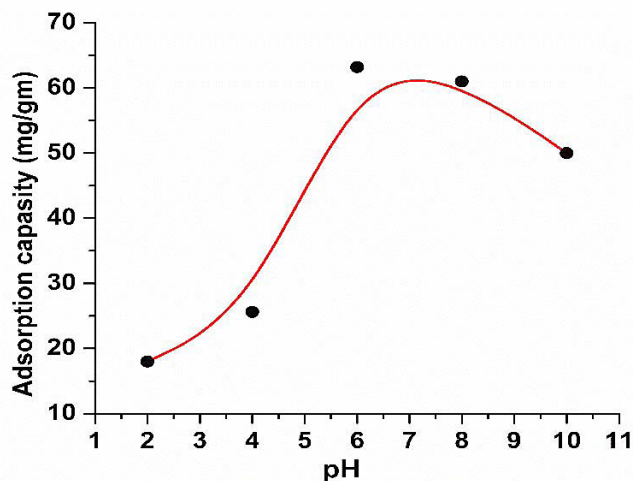


Fig. 4: Effect of Solution pH

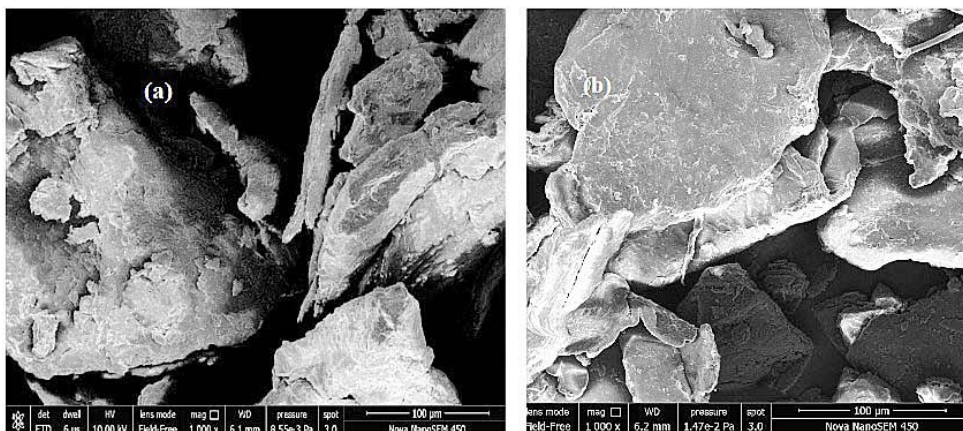


Fig. 5: FESEM images (a) TC-CS before and (b) after adsorption of lead

**Adsorption Isotherm Study**

Isotherm study delivers information about the applicability of the prepared adsorbent. It described the interaction of adsorbate with adsorbent. Certain sets of constant parameters which represent about the binding attraction of the adsorbent and may be used to assess the adsorbent’s adsorptive capacities for adsorbate molecules make up adsorption. A mathematical analysis of the equilibrium sorption/ aqueous concentration connection may be done using the Freundlich and Langmuir models.

**Freundlich Isotherm Model**

This theory is used to explain the interactions between adsorbed particles and the formation of multilayer adsorption with varying energies, which occur during adsorption on heterogenous surfaces.<sup>26</sup> According to this, adsorbate’s concentration on the adsorbent layer starts to increases as adsorbate concentration grows, and the sorption energy decreases exponentially after the adsorbent’s sorption centres are fully developed.

Non-Linear equation for Freundlich isotherm explains the link for both the amount of a substance adsorbed onto a surface and the equilibrium concentration of that substance in the surrounding solution<sup>27</sup> (Equation No.5).

$$q_e = K_F C_e^{1/n} \quad \dots(5)$$

Here  $q_e$  is stated as adsorption capacity ( in mg/g) and defined as the portion of fluoride adsorbed taken up by unit mass of adsorbent.  $C_e$  is remnant toxicant content left (mg/L) after equilibrium. Parameter  $n$  is related to quantify the strength of an adsorption force and  $K_F$  ((mg/g) (L/ mg)<sup>1/n</sup>) is the Freundlich adsorption constant concern with interfacial energy.

Adsorption strength ( $n$ ) refers to the amount of a substance that is adsorbed onto a surface per unit area which measures the intensity of adsorption. Chemical, linear, or physical adsorption processes may be identified when  $n < 1$ ,  $n = 1$ , or  $n > 1$ . More than 1 implies probability for physical adsorption is likely to occur.<sup>21</sup>

Adsorption behaviour is shown to be in agreement with the Freundlich model, as seen in Figure 6 by a non-linear graph of  $q_e$  against  $C_e$ . Intercept and slope, which are needed to calculate the Freundlich constants  $K_f$  and  $1/n$  are displayed in Table 1. With  $n$  consistently less than 1, chemisorption adsorption

of metal ions on the adsorbent seems to be the most likely explanation.

### Langmuir Isotherm

According to the Langmuir theory, the surface of the adsorbent is evenly distributed with a finite number of active sites. As these binding surfaces have the consistence tendency towards a monomolecular layer, therefore, no interactions exist betwixt adsorbed molecules.<sup>28,29</sup> Langmuir adsorption, a method initially developed to analyse adsorption in the gas-solid phase,<sup>30</sup> may be used to assess and compare the adsorptive capacities of various adsorbents.

Here is non-linear form of Langmuir equation

$$q_e = \frac{q_{max} K_L C_e}{1 + K_L C_e} \quad \dots(6)$$

Where  $q_e$  is equilibrium quantity of metal adsorbed;  $C_e$  is lead concentration at equilibrium (mg/L),  $K_L$  is concerned with the affinity of solute at adsorbent defined as Langmuir constant (L/mg) and  $q_{max}$  is theoretical monolayer adsorption capability of the adsorbent (mg/gm). The value of  $K_L$  and  $q_{max}$  at series of temperatures were provided in Table 1. Figure 6 demonstrates characteristics nonlinear Langmuir isotherm curves at various temperatures.

**Table 1: Langmuir and Freundlich isotherm Parameters**

Temperature	Langmuir isotherm				Freundlich isotherm			
	Qmax (mg/gm)	$K_L$	R <sup>2</sup>	SSE	$K_f$ ((mg/g) (L/ mg) <sup>1/n</sup> )	$n$	R <sup>2</sup>	SSE
25	380	0.9	0.9589	0.0263	0.1098	0.0606	0.8608	0.2936
35	330	0.895	0.9891	0.0202	0.0668	0.763	0.8935	0.2782
45	278	0.769	0.9738	0.0163	0.04957	0.816	0.902	0.2545
55	259	0.699	0.9878	0.0104	0.03756	0.8283	0.9339	0.2201

The separating coefficient (or equilibrium parameter)  $R_L$ , which is a constant with no dimensions, may be used in the following expression to characterize the Langmuir isotherm (Eq. 7)

$$R_L = \frac{1}{1 + K_L C_o} \quad \dots(7)$$

Here  $C_o$  is the original fluoride amounts (mg/L) and  $K_L$  (L/mg) known as Langmuir constant. The value of  $R_L$  reveals whether the isotherm task is linear ( $R_L = 1$ ), irreversible ( $R_L = 0$ ), favourable ( $0 < R_L < 1$ ), or unfavourable ( $R_L > 1$ ).<sup>31</sup> The current research focuses on  $R_L$  values that fall somewhere in the

range of 0.092 to 0.359, which demonstrates that the material that has been developed is suitable.

The equilibrium constants for both isotherms in addition to the linear regression coefficient ( $R^2$ ) and sum of square errors (SSE) indicate that Langmuir experimental data fits better than the Freundlich having a greater extent of linear regression and lower SSE. Additionally, the clear reduction in  $q_{max}$  and  $K_L$  with higher temperature implies about exothermic nature of adsorption.

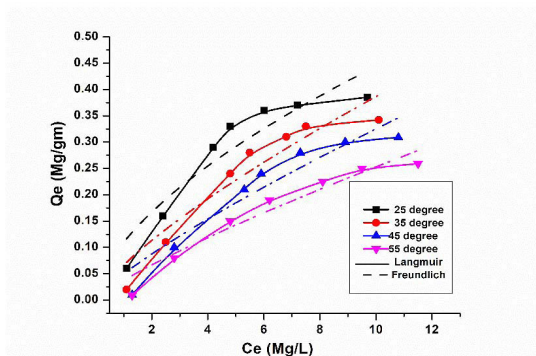


**Fig. 6: nonlinear adsorption isotherms for lead adsorption**

**Adsorption Kinetics**

The batch approach was used to investigate the kinetics characteristics for adsorption. In current finding, the pseudo-first and pseudo-second-order approach were used to estimate the sorption kinetics process.<sup>32,33</sup>

Following is the Pseudo-first order kinetic expression (equation no 8)

$$\text{Log}(q_e - q_t) = \text{Log}q_e - K_1 t/2.303 \quad \dots(8)$$

To anticipate the magnitude of  $K_1$  and  $q_e$  based on slope and intercept, a linear plot using  $\text{Log}(q_e - q_t)$  vs time was generated.

The slow rate of adsorption and the chemical nature of the adsorbent surface provide the basis for the pseudo-second-order hypothesis. It is possible to utilize Equation 9 as a representation of the pseudo-second-order kinetic model.

$$\frac{t}{q_t} = \frac{1}{K_2 q_e^2} + \frac{t}{q_e} \quad \dots(9)$$

The quantity of fluoride adsorbed (in mg/gm) at time  $t$  is referred to as  $q_t$ , while the amount at equilibrium time is termed as  $q_e$ . The pseudo-first order rate constant is denoted by  $K_1$ , whereas the pseudo-second order rate constant is denoted by  $K_2$ . The intercept of the  $(t/q_t)$  vs. time linear plot denotes  $K_2$ , whereas the slope denotes  $q_e$ .

Figures 7 and 8 depict the kinetic models for lead adsorption, whereas Table 2 lists the derived values. While the first-order model gives reasonable fitting with experimental findings, the second-order model demonstrates a superior description of lead adsorption onto thiocarbamoyl chitosan due to its smaller relative errors and greater degree of linear regression. Due to the calculated value's good agreement with the measured  $q_e$  value, the pseudo-second-order method seems to be accurate.

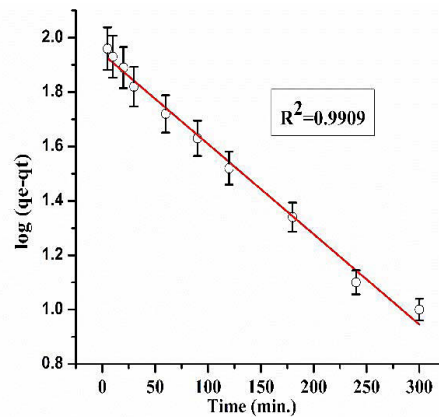


**Fig. 7: Pseudo first order study for lead removal**

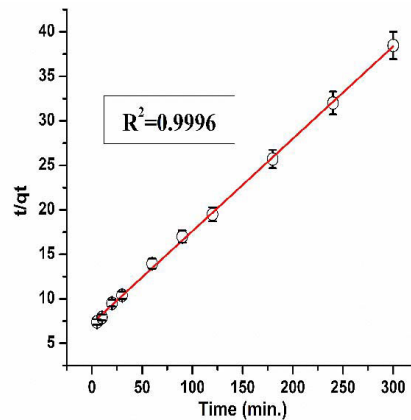


**Fig. 8: Pseudo second order study for lead removal**



**Table 2: Adsorption kinetics model for lead adsorption on TCCS**

Metal ion	Pseudo first order				Pseudo second order			
	$K_1$ min. <sup>-1</sup>	$q_e$ (mg/gm)	$R^2$	SSE	$K_2$ gm/LMin <sup>-1</sup>	$q_e$ (mg/gm)	$R^2$	SSE
Pb <sup>+2</sup>	0.0007	8.709	0.9903	0.8277	0.001476	9.78	0.9996	0.00858

**Thermodynamic Studies**

It has been determined that several thermodynamic factors, including  $\Delta G^\circ$  (standard free energy),  $\Delta H^\circ$  (enthalpy change), and  $\Delta S^\circ$  (entropy change), control the viability and makeup of the adsorption process. For computations, experimental data collected at various temperatures was utilised.

The van't Hoff equation was used to evaluate  $K_L$  value at varying temperatures.<sup>34</sup>

$$\ln K_L = \frac{\Delta S^\circ}{R} - \frac{\Delta H^\circ}{RT} \quad \dots(10)$$

Where  $\Delta H^\circ$  and  $\Delta S^\circ$  are changes in standard enthalpy and entropy respectively and R is the

universal gas constant and T is absolute temperature in kelvin. By plotting a graph between  $\ln K_L$  and  $1/T$ , a straight line curve is obtained (Figure 9) with intercept and slope equal to  $\Delta S^\circ/R$  and  $-\Delta H^\circ/R$ , respectively.

Gibbs energy change of activation can be computed from equation (11) and the obtained values of thermodynamic standards are summarised in Table 3.

$$\Delta G^\circ = \Delta H^\circ - T\Delta S^\circ \quad \dots(11)$$

**Table 3: Thermodynamic standards for lead adsorption on TCCS**

T (kelvin)	$\Delta G^\circ$	$T\Delta S^\circ$	$\Delta H^\circ$	$\Delta S^\circ$
298	-8.44	8.45		
308	-8.730	8.74	-0.09	0.028
318	-9.020	9.03		
328	-9.300	9.31		

As shown in Table 3, the exothermic character of the adsorption procedure is revealed by negative inputs of enthalpy changes. The positive value of entropy change demonstrated the increase in randomness at the solid-solution interface throughout the adsorption process.

A negative value of free energies suggested an energetically advantageous and reflected as the extent of the spontaneity of the adsorption process. The adsorption was more favourable at high temperatures, as seen by the larger negative free energy changes with increasing temperature. Overall, the negative free energy change values reflect the feasibility of the adsorbent and spontaneity of the adsorption process.<sup>35</sup>

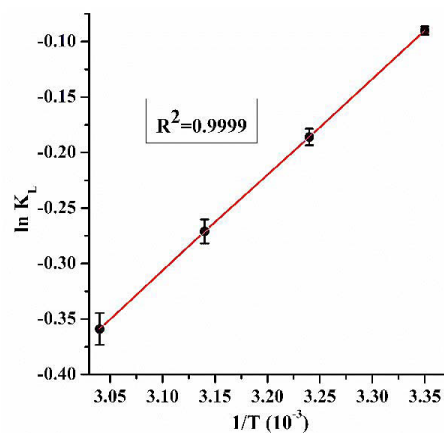


**Fig. 9: Van't Hoff plot for adsorption of lead**

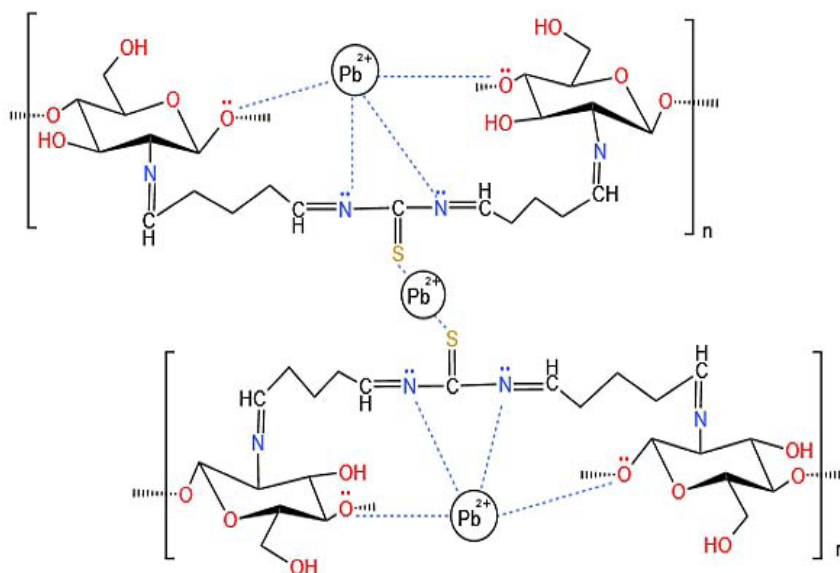


**Fig. 10: Mechanism for Lead adsorption by TCCS**

#### Adsorption Mechanism for the lead on TCCS Template

The possible site for cationic lead ion on to the prepared TCCS template in this study may be expected at nitrogen atoms of amino groups, sulphur atoms of thiocarbamoyl chitosan, and oxygen groups of the hydroxyl groups. The complexation of lead ion is illustrated in Figure 10. Electrostatic attraction between lone pair electrons of nitrogen and oxygen may be responsible for the complex formation. Sulphur atoms is considered as soft base according to HSAB concept and this will attempt to form stable complex with soft acid like lead ions.

#### Conclusion

In the undergoing study, the ability of chemically modified Chitosan (TC-CS) was evaluated for adsorbing noxious  $Pb^{2+}$  ions from an aqueous solution. Presence of other ions in removing lead depends on various factors such as concentration of ions, pH, temperature, the nature of the waste, and the treatment process being used. Nonetheless, class 'b' ( $Pb^{2+}$ ) and borderline ( $Zn^{2+}$ ,  $Cd^{2+}$ ,  $Cu^{2+}$ ,  $Co^{2+}$ , and  $Ni^{2+}$ ) metals do not seem to compete for binding sites.<sup>36</sup> Langmuir and Freundlich isotherms were described to simulate the adsorption process, along with kinetic and thermodynamic analyses. A pseudo-second-order approach was the most accurate description of the process. In addition, the

process was exothermic and highly spontaneous in view of negative free energy values. Langmuir model was considered as the best explained model rather than Freundlich model with higher linear regression. The findings of the batch adsorption investigation revealed that the removal effectiveness was at an all-time high rate of 85.86 percent in the slightly acidic region (pH=6). Thiocarbamoyl chitosan, once manufactured, has a high adsorption capacity (38 mg/gm), making it an appealing tool for cleansing lead-contaminated industrial waste streams.

#### Acknowledgement

Sardar Singh Poonia want to express his sincere gratitude towards CSIR (award no: 09/098 (0142)/2019-EMR-I) for providing support and financial aids in research. He would like to give special thanks to Department of Chemistry for their exceptional support for providing the necessary resources.

#### Funding

Sardar Singh Poonia want to express his sincere gratitude towards CSIR (award No: 09/098 (0142)/2019-EMR-I) for providing support and financial aids in research.

#### Conflict of interest

None

## References

1. Gupta K, Gusain R, Joshi P, Khatri O P. Adsorptive removal and photocatalytic degradation of organic pollutants using metal oxides and their composites: A comprehensive review. *Advances in colloid and interface science*. 2019; 272;102009.
2. Gao B, He F, Huang J, Jiang Y, Ok Y S, Wang H, Wan Y, Yang X, Yu Z, Zheng Y. Surface functional groups of carbon-based adsorbents and their roles in the removal of heavy metals from aqueous solutions: A critical review. *Chem. Eng. J.* 2019; 366;608–621.
3. Fernandez C. A. and Miretzky, P. 2009. Hg (II) removal from water by chitosan and chitosan derivatives: A review. *Journal of Hazardous Materials*, 167, 10–23.
4. US geological survey report on mineral commodity summaries, 2022 <https://pubs.usgs.gov/periodicals/mcs2022/mcs2022-lead.pdf>
5. Xie Y, Giammar D E. Effects of flow and water chemistry on lead release rates from pipe scales. *Water Res.* 2011; 45; 6525–6534.
6. Nordberg GF, Fowler BA, Nordberg M, Friberg LT, (eds.), *Introduction-General Considerations and International Perspectives*. In: *Handbook on the Toxicology of Metals*. 3rd edition. US; academic press, 2007;1-9.
7. Kaushik C P, Kaushi, N, Sharma JK. Studies on removal of Cr (VI) and Cu (II) ions using Chitosan, *Nat. Env. Polln. Tech.* 2005; 4(2), 163-166.
8. Regel M. A review on methods of regeneration of spent pickling solutions from steel processing. *Journal of hazardous material*. 2010; 177 (1-3); 57-69.
9. Huang Li, Huang wan, Shen R, Shuai Q. Chitosan/thiol functionalized metal–organic framework composite for the simultaneous determination of lead and cadmium ions in food samples. *Food Chemistry*, 2020;330;127212.
10. Ahmed M, Ahmad S, Ikram S. Chitosan: A Natural Antimicrobial Agent- A Review. *Journal of Applicable Chemistry*, 2014; 3(2); 493-503.
11. Ahmed S, Ikram S. Chitosan & its Derivatives: A Review in Recent Innovations. *International Journal of Pharmaceutical Research*, 2015; 6(1);14-30.
12. Cloirec PL, Coq L, Faur C, Nguyen TH, Phan NH, Rio S. Production of fibrous activated carbons from natural cellulose (jute, coconut) fibers for water treatment applications. *Carbon*. 2006; 44(12);2569–2577.
13. Ehara K, Kawamoto H, Saka S. Characterization of the lignin-derived products from wood as treated in supercritical water. *Journal of Wood Science*. 2002; 48; 320-325.
14. Robyt JF. Starch: Structure, Properties, Chemistry, and Enzymology. In: Bertram O. Fraser-Reid, Kuniaki Tatsuta, Joachim Thiem (Eds.) *Glycoscience*, Volume 1, 2nd edition, springer-verlag, 2008; 1438-1472.
15. Kumar P, Kadwasara A, Sharma P K, Choudhary A. Optimization of Adsorption Parameters For Removal Of Fluoride By Activated Carbon Prepared From Prosopis Cineraria Leaves. *Pollution Research*. 2021;40 (4);1424-1432.
16. Agarwal A, Vaishali. Chitosan Based Adsorbent: A Remedy to Handle Industrial Waste Water. *The International Journal of Engineering and Science*. 2017; 6 (9); 34-49.
17. Lei Z, Yuexian Z, Zehngjun C. Removal of heavy metal ions using chitosan and modified chitosan: A review. *Journal of Molecular Liquids*, 2016; 214; 175-191.
18. Pearson RG. Hard and Soft Acids and Bases. *J. Am. Chem. Soc.* 1963; 85; 3533-3539.
19. Sankararamakrishnan N, Sanghi R. Preparation and characterization of a novel xanthated chitosan. *Polymers*, 2006; 66; 160–167.
20. Pengcheng li, Huahua Yu, wang li, Kecheng Li, Rong X, Rongfeng Li, Song Liu, Yukun Qi. Studies on adsorption behaviour of Pb(II) onto a thiourea-modified chitosan resin with Pb(II) as template, *Carbohydrate Polymer*, 2010;81; 305.
21. Bhangar MI, Shahabuddin M, Solangi IB. Removal of fluoride from aqueous environment by modified Amberlite resin. *J. Hazard Mater*, 2009; 171(1–3); 815–819.

22. Dai J, Tao C, Ren F. Adsorption Behaviour of Fe(II) and Fe(III) Ions on Thiourea Cross-Linked Chitosan with Fe(III) as Template. *Molecules*. 2012; 17; 4388-4399.
23. Choudhary A, Kumar P, Kadawasara A, Poonia SS. 2022. Facile One Pot Synthesis of Thiocarbamoyl Chitosan for the Adsorptive Elimination of Hexavalent Cr (VI) Ions. *Res. J. Chem. Environ.* 2022; 26 (5);126-135.
24. Najafpoura GD, Ghoreyshi AA, Radnia H, Younesi H. Adsorption of Fe(II) ions from aqueous phase by chitosan adsorbent: equilibrium, kinetic, and thermodynamic studies *Desalination and water treatment*, 2012; 50; 348-359.
25. Wang Li, Xing R, Song Liu, Qin Yu, Li K, Yu H, Li R, Li P. Studies on adsorption behaviour of Pb(II) onto a thiourea-modified chitosan resin with Pb(II) as template. *Carbohydrate Polymers*. 2010; 81; 305–310
26. Ahmet S, Caner N, and Mustafa T. Adsorption Characteristics of Mercury (II) Ions from Aqueous Solution onto Chitosan-Coated Diatomite. *Ind. Eng. Chem. Res.* 2015; 54 (30); 7524–7533.
27. Freundlich H.M. über die adsorption in lösungen. *Zeitschrift für Physikalische Chemie (leipzig)*, 1906; 57A; 385–470.
28. Langmuir I. The constitution and fundamental properties of solids and liquids. *Journal of the Franklin Institute*, 1917;183(1);102–105.
29. Langmuir, I. *J. Am. Chem. Soc.* 1918; 40;1361
30. Elmorsi T. M. Equilibrium isotherms and kinetic studies of removal of methylene blue dye by adsorption onto miswak leaves as a natural adsorbent. *Journal of Environmental Protection*. 2011; 2(6); 817–827.
31. Acrivos A, Eagleton LC, Hall KR, Vermeulen T, Pore- and solid-diffusion kinetics in fixed-bed adsorption under constant-pattern conditions. *Ind. Eng. Chem. Fundamen.* 1966; 5(2); 212-223.
32. Lagergren S. Zur theorie der sogenannten adsorption geloster Stoffe. *Kungliga Svenska Vetenskapsakademiens, Handlingar*, 1898; 24; 1–39.
33. Ho Y S, McKay G. The kinetics of sorption of divalent metal ions onto sphagnum moss peat. *Water Research*, 2000;34(3); 735–742.
34. Tellinghuisen J. Van't Hoff analysis of  $K^{\circ}(T)$ :Howgood. or bad? *Biophysical Chemistry*, 2006; 120(2); 114–120.
35. Tahir SS, Rauf N. Thermodynamic studies of Ni(II) adsorption onto bentonite from aqueous solution. *J. Chem. Thermodynamics*, 2003; 35; 2003-2009.
36. Puranik, P.R. and Paknikar, K.M., Influence of co-cations on biosorption of lead and zinc-a comparative evaluation in binary and multi metal systems, *Bioresource Technology*, 1999; 70;269-276